

Selected Paper

Photocatalytic Overall Water Splitting on Gallium Nitride Powder

Kazuhiko Maeda,[1] Kentaro Teramura,[1] Nobuo Saito,[2] Yasunobu Inoue,[2] and Kazunari Domen*[1,3]

[1]Department of Chemical System Engineering, The University of Tokyo, 7-3-1 Hongo, Bunkyo-ku, Tokyo 113-8656

[2]Department of Chemistry, Nagaoka University of Technology, Nagaoka 940-2188

[3]Solution Oriented Research for Science and Technology (SORST) programs of the Japan Science and Technology Agency (JST), 4-1-8 Honcho, Kawaguchi 332-0012

Received October 16, 2006; E-mail: domen@chemsys.t.u-tokyo.ac.jp

Gallium nitride (GaN) powder was studied as a photocatalyst for overall water splitting. The photocatalytic activity of GaN for the reaction was found to be strongly dependent on the crystallinity of the material and the cocatalyst employed. Modification of well-crystallized GaN with $Rh_{2-y}Cr_yO_3$ nanoparticles as a cocatalyst for H_2 evolution resulted in the stable stoichiometric decomposition of H_2O into H_2 and O_2 under ultraviolet irradiation ($\lambda > 300$ nm) by the band gap transition. RuO_2 modification did not bring about appreciable H_2 and O_2 evolution. Low-crystallinity GaN exhibits negligible activity for overall water splitting, regardless of the kind of cocatalyst applied.

Photocatalytic overall water splitting for the production of hydrogen as a clean and renewable energy source using solar energy is an important and challenging topic. Non-oxide materials, such as oxysulfides and oxynitrides, are promising photocatalysts for overall water splitting under visible irradiation.[1–4] Although a large number of metal-oxides that function as a photocatalyst for the overall water splitting reaction has been developed to date,[5] such catalysts are not active in the visible region. However, there have been a few examples of non-oxide photocatalysts that are active for the reaction: β-Ge_3N_4,[6] $(Ga_{1-x}Zn_x)(N_{1-x}O_x)$,[3] Zn–Ge oxynitride,[4] and GaN doped with divalent cations (e.g., Mg^{2+} and Zn^{2+}).[7] The lack of suitable non-oxide catalysts suggests that it is considerably more difficult to achieve overall water splitting using such a material. The development of new non-oxide materials that exhibit activity for photocatalytic overall water splitting, particularly under visible irradiation, is therefore of significant interest in terms of both solar-driven photocatalysis and general progress in photocatalysis technology.

The present study focuses on gallium nitride (GaN) powder for use as a photocatalyst for overall water splitting. GaN is a technologically important material with a wurtzite crystal structure, in which GaN_4 tetrahedrons are corner-shared, as shown in Fig. 1.[8] Extensive research has been conducted into GaN for applications, such as light functional devices and photoelectrodes.[9,10] It is well known that GaN-based nitrides display intense emission in the ultraviolet–visible region, when employed as a light-emitting diode,[9] suggesting that the materials are promising for use as photocatalysts. Turner et al. have reported that Mg- or Si-doped GaN thin film, having p- or n-type semiconducting characteristics, respectively, exhibits band-edge potentials suitable for overall water splitting.[10] Overall water splitting reaction can be achieved using a photoelectrochemical cell consisting of photoanode of such a GaN thin film and a Pt cathode upon band gap illumination.[10] Our group has also recently reported that GaN powder doped with divalent cations displays activity for overall water splitting under ultraviolet (UV) irradiation ($\lambda > 300$ nm) when loaded with RuO_2 as a cocatalyst.[7] The same photocatalyst prepared without doping does not display activity for the reaction,[3a,7] and undoped GaN powder has yet to be reported to achieve overall water splitting regardless of modification.

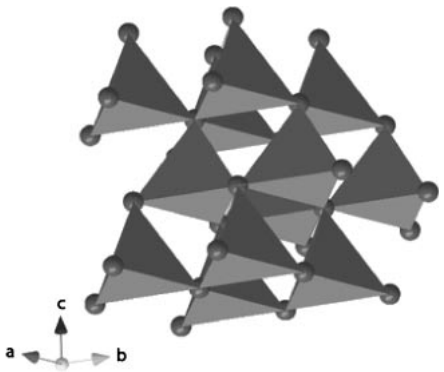

Fig. 1. Schematic illustration of wurtzite structure of GaN. Each tetrahedral unit indicates GaN_4 tetrahedron.

In this paper, undoped GaN powder modified with $Rh_{2-y}Cr_yO_3$ nanoparticles were shown to be active for photocatalytic water splitting under UV irradiation ($\lambda > 300$ nm). The effect of the crystalline properties of the GaN powder on catalytic performance and the role of $Rh_{2-y}Cr_yO_3$ nanoparticles as efficient H_2 evolution sites were examined, and the essential requirements for overall water splitting using GaN powder are discussed in detail.

Experimental

Materials. Two types of GaN powder were examined as photocatalysts for overall water splitting: GaN prepared from elemental gallium (Mitsubishi Chemicals), and GaN prepared by nitridation of Ga_2O_3 powder (High Purity Chemicals, 99.9%) under NH_3 flow at 1123 K for 15 h. These based powders are referred to here-

Published on the web May 14, 2007; doi:10.1246/bcsj.80.1004

after as GaN(MC) and GaN(HM), respectively.

Modification with $Rh_{2-y}Cr_yO_3$ or RuO_2 Nanoparticles. $Rh_{2-y}Cr_yO_3$ or RuO_2 nanoparticles as water splitting promoters were loaded onto the GaN powder according to the method reported previously.[3] In the case of $Rh_{2-y}Cr_yO_3$, GaN powder and an aqueous solution containing an appropriate amount of $Na_3RhCl_6 \cdot 2H_2O$ (Kanto Chemicals, 97% as Rh) and $Cr(NO_3)_3 \cdot 9H_2O$ (Wako Pure Chemicals, 99.9%) were placed in an evaporating dish in a water bath. The suspension was stirred to complete evaporation using a glass rod. The resulting powder was collected and heated in air at 623 K for 1 h to convert the Rh and Cr species to $Rh_{2-y}Cr_yO_3$.[3f] The catalyst was loaded with 1 wt % Rh and 1.5 wt % Cr (metallic content), which has previously been found to be optimal in the case of $(Ga_{1-x}Zn_x)(N_{1-x}O_x)$, a visible-light-driven photocatalyst for overall water splitting.[3] Prior to photocatalytic reactions, the $Rh_{2-y}Cr_yO_3$-loaded GaN was washed with distilled water to remove any remaining impurities, e.g., Na^+, Cl^-, Cr^{6+}, from the catalyst surface.[3f] To load the catalyst with RuO_2, the GaN powder was immersed in a tetrahydrofuran (THF) solution containing dissolved $Ru_3(CO)_{12}$ (Aldrich Chemical Co., 99%) and stirred at 333 K for 5 h. The solution was then dried under reduced pressure by heating in air at 373 K for 1 h to remove THF. The resulting powder was finally heated in air at 623 K for 1 h to convert the Ru species to RuO_2.[3c] The amount of loaded RuO_2 was 5 wt %.

Characterization of Catalysts. The samples were studied by powder X-ray diffraction (XRD; RINT-UltimaIII, Rigaku; Cu Kα), scanning electron microscopy (SEM; S-4700, Hitachi), UV–visible diffuse reflectance spectroscopy (DRS; V-560, Jasco), and X-ray photoelectron spectroscopy (XPS; ESCA-3200, Shimadzu). The UV–visible DR spectra were converted from reflectance to absorbance by the Kubelka–Munk method. A $BaSO_4$ plate was used as a reference to correct the spectra. The binding energies determined by XPS were corrected in reference to the $Au4f_{7/2}$ peak (83.8 eV) for each sample. The chemical composition of the materials was determined by inductively coupled plasma optical emission spectroscopy (ICP-OES; Iris Advantage Duo, Thermo Elemental Co.) and a TC436 oxygen and nitrogen determinator (LECO Corporation). The Brunauer–Emmett–Teller (BET) surface area was measured using a BELSORP-mini instrument (BEL Japan) at liquid nitrogen temperature.

Photocatalytic Reactions. Reactions were carried out in a Pyrex inner irradiation-type reaction vessel connected to a glass-closed gas circulation and evacuation system. The overall water splitting reaction was performed in an aqueous H_2SO_4 solution containing 0.3 g of the catalyst. The pH of the reactant solution was adjusted to 3.0 in the case of the RuO_2-loaded sample and 4.5 for the $Rh_{2-y}Cr_yO_3$-loaded sample according to previous optimizations of reactions conditions for $(Ga_{1-x}Zn_x)(N_{1-x}O_x)$.[3a,e] The reactant solution was evacuated several times prior to the start of reaction to ensure complete air removal, and then the vessel was irradiated at $\lambda > 300$ nm using a 450-W high-pressure Hg lamp (UM-452, Ushio). Photocatalytic half reactions, that is, photoreduction of H^+ to H_2 in aqueous methanol solution (10 vol %) and photooxidation of H_2O to O_2 in aqueous silver nitrate solution (0.01 M), were also performed in the same manner. The temperature of the reactant solution was maintained at 293 ± 5 K by flowing water during the reaction. The evolved gases were analyzed by gas chromatography.

The quantum efficiency (Φ) was estimated by the method described previously[3a] using the equation $\Phi[\%] = (2 \times R/I) \times 100$, where R and I represent the number of evolved H_2 molecules and the number of incident photons. Here, Φ is the quantum efficiency assuming all incident photons are absorbed by the photocatalyst. The number of incident photons was measured using a calibrated Si photodiode.

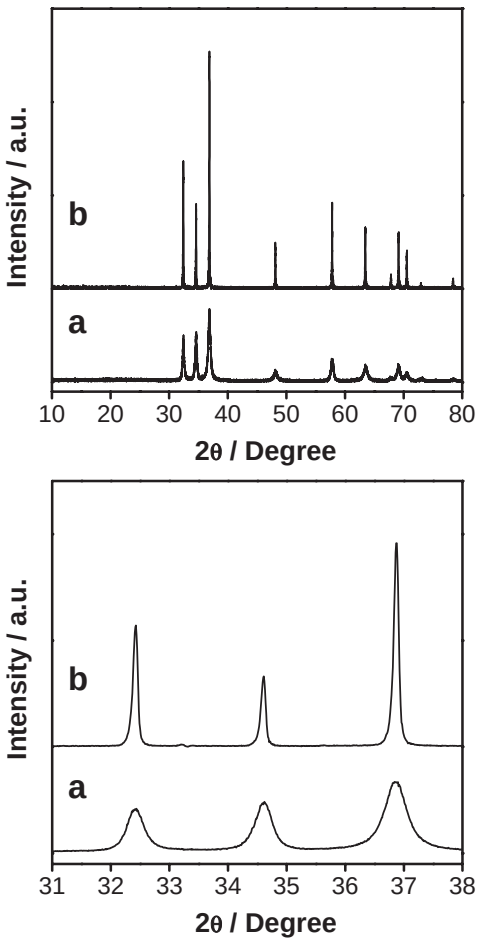

Fig. 2. Powder XRD patterns for GaN: (a) GaN(HM) and (b) GaN(MC).

Results and Discussion

Crystal Structure and Electron Microscopy. Powder XRD patterns of the two GaN powders are shown in Fig. 2. Both samples exhibited single-phase diffraction patterns, which are indicative of a hexagonal wurtzite structure,[8] with no peaks assignable to gallium oxide or hydroxide. The diffraction peaks for GaN(MC) were much narrower and more intense than those for GaN(HM), suggesting that GaN(MC) has a higher crystallinity.

Figure 3 shows the corresponding SEM images. The morphologies of the two GaN powders differed considerably in that GaN(HM) forms large agglomerates consisting of small primary particles (0.1–0.2 μm), while GaN(MC) has a smooth surface consisting of larger primary particles (0.5–2 μm) and secondary particles. These observations are consistent with the XRD measurements (Fig. 2). The specific surface areas of GaN(HM) and GaN(MC) were calculated to be 6.8 and 0.3 $m^2 g^{-1}$, respectively.

XPS. The surface electronic state of the two types of GaN was investigated by XPS. Figure 4 shows the XPS spectra for

the $Ga2p_{3/2}$, O1s, and N1s peaks in GaN. No appreciable differences in peak positions were observed between GaN(MC) and GaN(HM). The position of the $Ga2p_{3/2}$ peak was observably higher than the reported values for GaN thin film (1117.1 eV,[11] 1118.0 eV[12]), which is attributed to the greater abundance of oxygen species on the surface, as can be seen in the O1s spectra.[11] The O1s peaks for both GaN powders could be resolved into 2 peaks (530.9–531.3 and 532.1–532.6 eV) assignable to lattice oxygen and surface OH groups, respectively. The N1s peak position is close to that reported previously for N1s in GaN (397.3 eV,[12] 397.8 eV[13]). However, the intensity of the N1s peak for GaN(HM) was somewhat smaller than that for GaN(MC) due to the presence of oxygen species. As can be seen in the O1s spectra, the intensity of the O1s peak assigned to lattice oxygen for GaN(HM) was also somewhat larger than for GaN(MC), indicating that the GaN(HM) surface hosts a higher concentration of oxygen compared to the GaN(MC) surface.

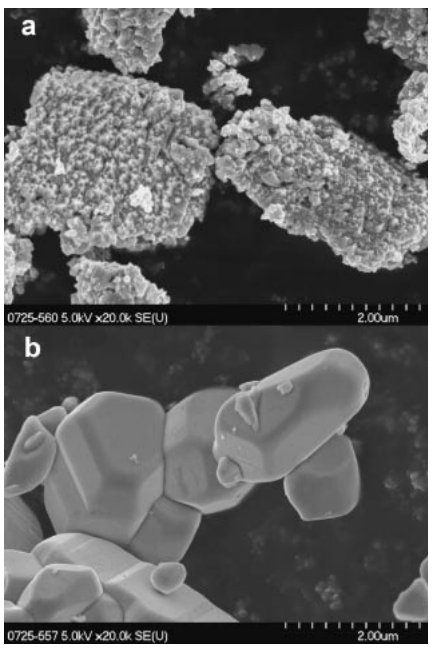

Fig. 3. SEM images of GaN powder: (a) GaN(HM) and (b) GaN(MC).

Atomic Compositions. Table 1 shows the bulk and surface atomic compositions (O/Ga and N/Ga) for GaN. The bulk atomic ratios were determined by elemental analysis, and the surface ratios were estimated from the areas of the O1s, N1s, and $Ga2p_{3/2}$ peaks in the XPS spectra. The atomic ratio of N/Ga in GaN(MC) was 1.0, indicating stoichiometry. Although surface oxygen species were detected by XPS (Fig. 4), the amount of oxygen in the GaN(MC) bulk was found to be negligible. In contrast, the atomic ratio of N/Ga in the GaN(HM) bulk was clearly less than unity, and the amount of oxygen both in the bulk and on the surface was greater than that for GaN(MC). These results indicate that the density of defect sites in the GaN(HM) bulk is substantially higher than in GaN(MC), even though the two powders have the same wurtzite crystal structure (Fig. 2).

UV–Visible Diffuse Reflectance Spectra. Figure 5 shows the UV–visible DRS results for the two GaN samples. GaN(MC) exhibited a steep absorption edge at ca. 380 nm and a long tail in the visible region. The position of the absorption edge of GaN(MC) was located at a slightly longer wavelength than those of a bulk-type GaN film[14a] and a GaN single crystal[14b] reported previously. An apparent red shift observed in the present case is presumably due to the difference in the form of GaN and the method for the measurement. In addition, the existence of a broad absorption in the visible region ($\lambda > 400$ nm) might cause the position of the real absorption edge to be ambiguous.

Table 1. Bulk and Surface Atomic Compositions of GaN

Sample	Bulk atomic ratio[a)]		Surface atomic ratio[b)]	
	N/Ga	O/Ga	N/Ga	O[c)]/Ga
GaN(HM)	0.9	0.2	0.3	0.6
GaN(MC)	1.0	$\ll$0.01	0.7	0.4

a) Determined by ICP-OES. b) Estimated from corresponding XPS peak areas. c) O1s peak assignable to lattice oxygen.

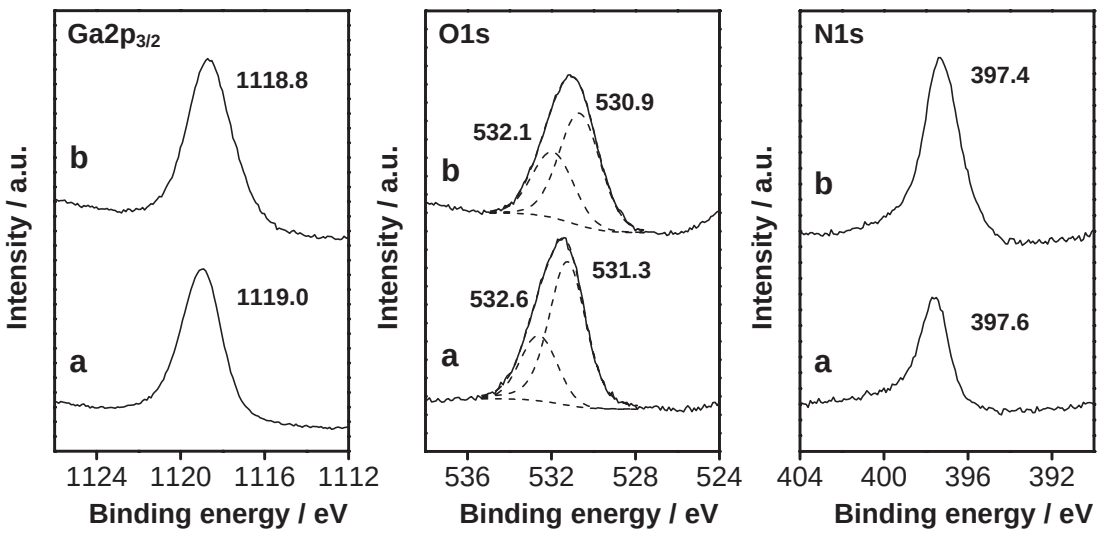

Fig. 4. XPS spectra for $Ga2p_{3/2}$, O1s, and N1s of GaN: (a) GaN(HM) and (b) GaN(MC).

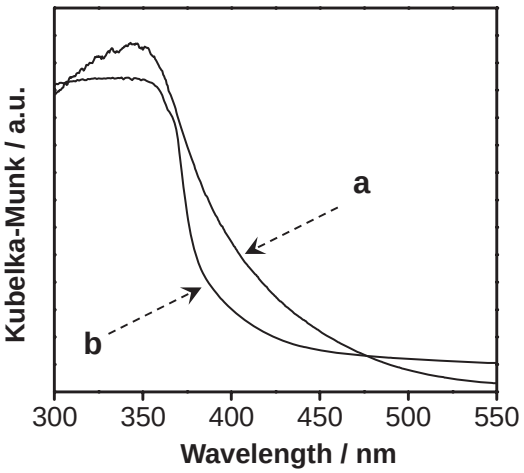

Fig. 5. Diffuse reflectance spectra for GaN: (a) GaN(HM) and (b) GaN(MC).

Table 2. Photocatalytic Activities of GaN for H_2 or O_2 Evolution in the Presence of Sacrificial Reagents under UV Irradiation ($\lambda > 300$ nm)[a)]

Sample	Reactant solution	Activity/μmol h^{-1}	
		H_2[c)]	O_2[d)]
GaN(HM)[b)]	10 vol % MeOH aq.	18	—
GaN(MC)[b)]	10 vol % MeOH aq.	90	—
GaN(HM)	0.01 M $AgNO_3$ aq.	—	214
GaN(MC)	0.01 M $AgNO_3$ aq.	—	704

a) Catalyst (0.3 g); an aqueous solution (370 mL); light source, high-pressure mercury lamp (450 W); inner irradiation-type reaction vessel made of Pyrex. b) Loaded with $Rh_{2-y}Cr_yO_3$. c) Steady rate of gas evolution. d) Initial rate of gas evolution.

As reported in the previous paper,[3b] density functional theory (DFT) calculations show that the tops of the valence bands for GaN are composed of N2p orbitals, whereas the bottoms of the conduction bands consist of 4s,4p hybridized orbitals of Ga. Therefore, the absorption band around 380 nm was attributed to the transition from N2p orbitals to hybridized Ga4s,4p orbitals. The broad absorption in the visible region is probably due to remnant Ga. The spectrum for GaN(HM) included a shoulder peak at a wavelength of ca. 400–500 nm, presumably due to nitrogen defects in the GaN(HM) bulk, as suggested above.

Photocatalytic Activities for H_2 or O_2 Evolution in the Presence of Sacrificial Reagents. Prior to the overall water splitting reactions, the individual photocatalytic activities for H_2 and O_2 evolution in the presence of a sacrificial electron donor or acceptor were investigated. Reactions involving sacrificial reagents are not "overall" water splitting reactions, but are often carried out as test reactions for overall water splitting.[5b] As GaN(HM) and GaN(MC) without modification displayed no activity for H_2 evolution even in the presence of methanol as a sacrificial electron donor, the $Rh_{2-y}Cr_yO_3$-loaded catalysts were used to ensure promotion of H_2 evolution.[3d–f] As shown in Table 2, both GaN(HM) and GaN(MC) exhibited activity for both H_2 and O_2 evolution, indicating that GaN meets the thermodynamic requirement for overall water splitting, that is, the tops of valence bands of the material are located at a more positive level than the water oxidation potential, whereas the bottoms of the conduction bands are located at a more negative level than the water reduction potential. However, the activities for H_2 evolution were approximately an order of magnitude lower than for O_2 evolution, and GaN(MC) exhibited higher activities than GaN(HM).

Table 3. Photocatalytic Activity of GaN for Overall Water Splitting under UV Irradiation ($\lambda > 300$ nm)[a)]

Sample	Cocatalyst	Activity[b)]/μmol h^{-1}		
		H_2	O_2	N_2
GaN(HM)	None	0	0	0
GaN(HM)	RuO_2	0	0	0
GaN(HM)	$Rh_{2-y}Cr_yO_3$	0.4	0	0.6
GaN(MC)	None	0	0	0
GaN(MC)	RuO_2	4.2	0	1.9
GaN(MC)	$Rh_{2-y}Cr_yO_3$	19	9.5	0

a) Catalyst (0.3 g); an aqueous solution (370 mL); light source, high-pressure mercury lamp (450 W); inner irradiation-type reaction vessel made of Pyrex. b) Steady rate of gas evolution.

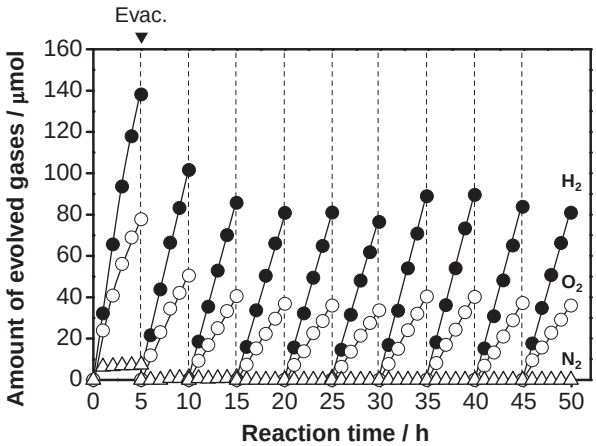

Fig. 6. Time course of overall water splitting over GaN(MC) under UV irradiation ($\lambda > 300$ nm). Reaction conditions: 0.3 g of catalyst, aqueous solution adjusted to pH 4.5 with H_2SO_4 (370 mL), high-pressure mercury lamp (450 W), Pyrex inner irradiation-type reaction vessel.

Photocatalytic Activity for Overall Water Splitting. Table 3 lists the photocatalytic activity of GaN modified with RuO_2 or $Rh_{2-y}Cr_yO_3$ for overall water splitting under UV irradiation ($\lambda > 300$ nm). None of the RuO_2-loaded or unmodified cocatalysts exhibited activity for simultaneous H_2 and O_2 evolution under these conditions. Over RuO_2-loaded GaN(MC), N_2 was evolved instead of O_2, indicating that the photogenerated holes oxidize not water molecules but the catalyst itself by the reaction $2N^{3-} + 6h^+ \rightarrow N_2$.[2a–d,3b,e] However, the $Rh_{2-y}Cr_yO_3$-loaded GaN(MC) displayed clear stoichiometric H_2 and O_2 evolution. A typical time course for overall water splitting on $Rh_{2-y}Cr_yO_3$-loaded GaN(MC) under UV irradiation ($\lambda > 300$ nm) is shown in Fig. 6. The reaction was continued for 50 h with evacuation every 5 h to evaluate the stability of the catalyst. The rates of H_2 and O_2 evolution decreased gradually with each reaction run of 5 h, but reached an almost constant level after approximately 15 h, yielding stable perform-

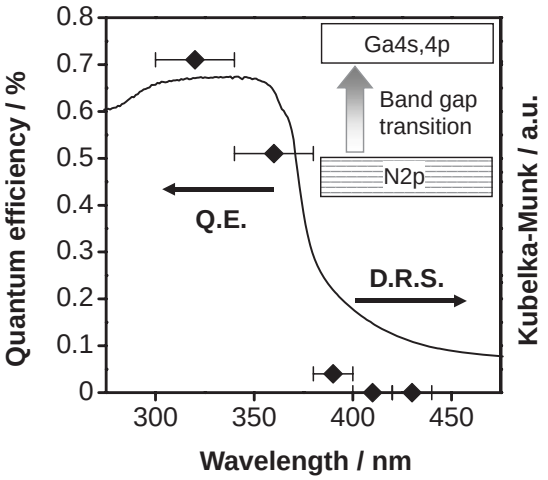

Fig. 7. Apparent quantum efficiency of $Rh_{2-y}Cr_yO_3$-loaded GaN(MC) for overall water splitting as a function of wavelength of incident light. Reaction conditions: 0.8 g of catalyst, aqueous solution adjusted to pH 4.5 with H_2SO_4 (100 mL), xenon lamp (300 W) with cutoff filter, Pyrex top irradiation-type reaction vessel.

ance for an extended reaction period. A low level of N_2 evolution (ca. 10 μmol) was detected in the initial stage of the reaction (0–15 h), which was attributed to oxidation of N^{3-} species near the GaN surface to N_2, as mentioned above. However, the production of N_2 was completely suppressed after repeated runs and no noticeable change in the XRD patterns was observed even after 50 h of reaction, demonstrating the stability of the material.

The quantum efficiency of $Rh_{2-y}Cr_yO_3$-loaded GaN(MC) for overall water splitting as a function of irradiation wavelength is shown in Fig. 7.[15] The apparent quantum efficiency decreased with increasing cutoff wavelength, and the onset wavelength was found to be consistent with that indicated by the diffuse reflectance spectrum. Irradiation at wavelengths longer than 400 nm did not produce appreciable conversion. These results clearly indicated that the reaction proceeded photocatalytically via the band gap transition from the valence band formed by N 2p orbitals to the conduction band formed by Ga4s,4p hybridized orbitals. Sakata et al. have reported that Ga_2O_3, a typical metal-oxide photocatalyst, exhibits activity for overall water splitting when loaded with NiO as a cocatalyst but only at UV wavelengths shorter than 275 nm due to the large band gap energy of the material (ca. 4.5 eV).[5f] Accordingly, it is clear that the main unit of active sites for overall water splitting in GaN is not Ga–O species on the surface but the GaN_4 tetrahedra unit constituting the wurtzite crystal structure.

The apparent quantum efficiency of the present $Rh_{2-y}Cr_yO_3$-loaded GaN(MC) (ca. 0.7% at 300–340 nm) is about an order of magnitude lower than those of the same non-oxide photocatalysts, e.g., $Rh_{2-y}Cr_yO_3$-loaded $(Ga_{1-x}Zn_x)(N_{1-x}O_x)$ (ca. 4% at 300–340 nm)[3d] and RuO_2-loaded Ge_3N_4 (ca. 9% around 300 nm.[6] As mentioned above, GaN(MC) had a specific surface area of 0.3 $m^2\,g^{-1}$, which is smaller than those of $(Ga_{1-x}Zn_x)(N_{1-x}O_x)$ (7.4 $m^2\,g^{-1}$, $x = 0.12$)[3b] and Ge_3N_4 (2.4 $m^2\,g^{-1}$). Therefore, it is likely that the relatively low quantum efficiency of the present catalyst is due to the small surface area. In metal-oxide photocatalysts, it has been reported that a decrease in the surface area of the catalyst directly contributes to a decrease in the activity, because the number of the surface reaction sites becomes small.[5a,d,e] The fact that the loading amount of $Rh_{2-y}Cr_yO_3$ cocatalysts has not been optimized would also have a negative effect on the quantum efficiency. Accordingly, the performance of GaN is expected to be improved by developing a new preparation method that can produce a material with high crystallinity and large surface area as well as refining the loading amount of cocatalysts.

Factors Governing Photocatalytic Activity. The characterization results above suggest that the physicochemical properties of GaN(HM) and GaN(MC) are dissimilar. GaN(MC) was highly crystalline, as indicated by XRD measurements and SEM observations, while GaN(HM) appeared to have low crystallinity considering the relatively high density of defect sites in the bulk. Consistent with these observations, GaN(MC) exhibited higher photocatalytic activity both for half reactions (H_2 and O_2 evolution) in the presence of sacrificial reagents (Table 2) and in overall water splitting (Table 3). The high crystallinity of GaN(MC) allows electrons and holes photogenerated in the catalyst bulk to migrate to the surface reaction sites with less recombination, leading to higher photocatalytic activity. On the other hand, recombination between photogenerated electrons and holes would occur frequently both in the bulk and on the surface of GaN(HM) due to the high density of nitrogen vacancies in the crystal and the rough surface structure. The specific surface area of GaN(HM) is approximately 23 times that of GaN(MC), and the number of reaction sites on the surface is expected to be similarly higher. In this case, however, it is clear that the crystallinity is of particular importance for obtaining high photocatalytic activity for the water splitting reaction.

The difference in crystallinity is also apparent in the activities for H_2 and O_2 evolution in the presence of sacrificial reagents. As shown in Table 2, the activities of both GaN(MC) and GaN(HM) for H_2 evolution were about an order of magnitude lower than for O_2 evolution, and the difference in activity between GaN(MC) and GaN(HM) was larger for H_2 evolution than for O_2 evolution. Specifically, GaN(MC) exhibited five times higher activity than GaN(HM) in the H_2 evolution reaction, yet only 3.5 times higher activity in the O_2 evolution reaction. This result showed that the migration of photogenerated electrons from the bulk to the surface is more severely obstructed in GaN(HM) than the migration of photogenerated holes. Elemental analysis (Table 1) showed that GaN(HM) contains many nitrogen vacancies in the crystal, which would produce large band bending at the solid–liquid interface, thus forming a Schottky barrier.[16] The large band bending in the GaN(HM) is expected to hinder prompt electron migration from the bulk to the surface, degrading the activity for water reduction. The relatively low activity for H_2 evolution compared to O_2 evolution is a common characteristic of (oxy)-nitride-type photocatalysts[2,3d] and is considered to be caused by the higher donor concentration in the material.

Although both GaN(HM) and GaN(MC) were confirmed to be active for H_2 or O_2 evolution in the presence of methanol or silver nitrate as sacrificial reagents (Table 2), overall

water splitting was achieved only over $Rh_{2-y}Cr_yO_3$-loaded GaN(MC). GaN(HM) exhibited negligible activity for overall water splitting even when modified with $Rh_{2-y}Cr_yO_3$ nanoparticles (Table 3). In overall water splitting, photogenerated electrons and holes in the bulk must migrate a relatively long distance to the surface reaction sites. The degree of crystallinity is thus the most important factor governing the performance of a catalyst in overall water splitting.

The activity of the loaded GaN(MC) photocatalyst for overall water splitting differed depending on the cocatalyst employed. RuO_2, which has been used as a cocatalyst for overall water splitting with many photocatalysts,[3a–c,4,5b–d,6,7] did not improve the activity of GaN(MC) for the splitting reaction, judging from the lack of O_2 evolution in the overall water splitting reaction (Table 3), as reported previously.[3a,7] Unmodified GaN(MC) exhibited no activity for H_2 evolution in the presence of methanol, but produced O_2 from aqueous silver nitrate solution (Table 2). Furthermore, as described above, loading cocatalysts is indispensable for achieving H_2 evolution from an aqueous methanol solution using GaN catalyst, indicating that GaN itself can oxidize methanol on its surface, but does not possess H_2 evolution sites. Taking these results into account, the rate-determining step for overall water splitting over GaN was considered to be the water reduction process by photogenerated electrons. As demonstrated in the previous study, $Rh_{2-y}Cr_yO_3$ nanoparticles are more efficient H_2 evolution sites than RuO_2.[3d,e] It is therefore considered that the superiority of $Rh_{2-y}Cr_yO_3$ nanoparticles as a cocatalyst for H_2 evolution mainly contributes to achieving the overall water splitting on GaN(MC). We have previously reported that GaN doped with divalent cations shows higher photocatalytic activity for overall water splitting than undoped GaN, even though there is no difference in crystallinity between doped and undoped GaN.[7] This is attributed to an increase in the mobility and concentration of holes due to the formation of acceptor level derived from the dopants.[7] Accordingly, to increase the number of photogenerated carriers available for the surface chemical reactions is essential for achieving overall water splitting using a GaN-based material.

Conclusion

GaN powder was confirmed to meet the thermodynamic requirements for overall water splitting and was demonstrated to function as a stable photocatalyst for overall water splitting under UV irradiation ($\lambda > 300$ nm), when modified with $Rh_{2-y}Cr_yO_3$ nanoparticles as a cocatalyst for H_2 evolution. The photocatalytic activity of GaN for overall water splitting was shown to depend strongly on the crystallinity of the material and the kind of cocatalyst applied. The crystallinity of GaN predominantly affected the efficiency of water photoreduction rather than water photooxidation. Modification of well-crystallized GaN with a superior cocatalyst that promotes H_2 evolution is concluded to be most important for achieving efficient overall water splitting.

The authors thank Ms. Y. Kako of the Department of Chemical System Engineering, The University of Tokyo, and the staff of the Institute for Materials Research, Tohoku University, for elemental analyses. This work was supported by the Solution Oriented Research for Science and Technology (SORST) program of the Japan Science and Technology (JST) Agency and the 21st Century Center of Excellence (COE) program of the Ministry of Education, Culture, Sports, Science and Technology of Japan.

References

1 a) A. Ishikawa, T. Takata, J. N. Kondo, M. Hara, H. Kobayashi, K. Domen, *J. Am. Chem. Soc.* **2002**, *124*, 13547. b) A. Ishikawa, Y. Yamada, T. Takata, J. N. Kondo, M. Hara, H. Kobayashi, K. Domen, *Chem. Mater.* **2003**, *15*, 4442. c) A. Ishikawa, T. Takata, T. Matsumura, J. N. Kondo, M. Hara, H. Kobayashi, K. Domen, *J. Phys. Chem. B* **2004**, *108*, 2637.

2 a) G. Hitoki, T. Takata, J. N. Kondo, M. Hara, H. Kobayashi, K. Domen, *Chem. Commun.* **2002**, 1698. b) G. Hitoki, A. Ishikawa, T. Takata, J. N. Kondo, M. Hara, K. Domen, *Chem. Lett.* **2002**, 736. c) A. Kasahara, K. Nukumizu, G. Hitoki, T. Takata, J. N. Kondo, M. Hara, H. Kobayashi, K. Domen, *J. Phys. Chem. A* **2002**, *106*, 6750. d) A. Kasahara, K. Nukumizu, T. Takata, J. N. Kondo, M. Hara, H. Kobayashi, K. Domen, *J. Phys. Chem. B* **2003**, *107*, 791. e) D. Yamasita, T. Takata, M. Hara, J. N. Kondo, K. Domen, *Solid State Ionics* **2004**, *172*, 591.

3 a) K. Maeda, T. Takata, M. Hara, N. Saito, Y. Inoue, H. Kobayashi, K. Domen, *J. Am. Chem. Soc.* **2005**, *127*, 8286. b) K. Maeda, K. Teramura, T. Takata, M. Hara, N. Saito, K. Toda, Y. Inoue, H. Kobayashi, K. Domen, *J. Phys. Chem. B* **2005**, *109*, 20504. c) K. Teramura, K. Maeda, T. Saito, T. Takata, N. Saito, Y. Inoue, K. Domen, *J. Phys. Chem. B* **2005**, *109*, 21915. d) K. Maeda, K. Teramura, D. Lu, T. Takata, N. Saito, Y. Inoue, K. Domen, *Nature* **2006**, *440*, 295. e) K. Maeda, K. Teramura, H. Masuda, T. Takata, N. Saito, Y. Inoue, K. Domen, *J. Phys. Chem. B* **2006**, *110*, 13107. f) K. Maeda, K. Teramura, D. Lu, T. Takata, N. Saito, Y. Inoue, K. Domen, *J. Phys. Chem. B* **2006**, *110*, 13753. g) K. Maeda, K. Teramura, N. Saito, Y. Inoue, K. Domen, *J. Catal.* **2006**, *243*, 303.

4 Y. Lee, H. Terashima, Y. Shimodaira, K. Teramura, M. Hara, H. Kobayashi, K. Domen, M. Yashima, *J. Phys. Chem. C* **2007**, *111*, 1042.

5 a) K. Domen, J. N. Kondo, M. Hara, T. Takata, *Bull. Chem. Soc. Jpn.* **2000**, *73*, 1307, and references therein. b) A. Kudo, *Catal. Surv. Asia* **2003**, *7*, 31, and references therein. c) J. Sato, N. Saito, H. Nishiyama, Y. Inoue, *J. Phys. Chem. B* **2001**, *105*, 6061. d) K. Ikarashi, J. Sato, H. Kobayashi, N. Saito, H. Nishiyama, Y. Inoue, *J. Phys. Chem. B* **2002**, *106*, 9048. e) J. Sato, H. Kobayashi, K. Ikarashi, N. Saito, H. Nishiyama, Y. Inoue, *J. Phys. Chem. B* **2004**, *108*, 4369. f) T. Yanagida, Y. Sakata, H. Imamura, *Chem. Lett.* **2004**, *33*, 726.

6 J. Sato, N. Saito, Y. Yamada, K. Maeda, T. Takata, J. N. Kondo, M. Hara, H. Kobayashi, K. Domen, Y. Inoue, *J. Am. Chem. Soc.* **2005**, *127*, 4150.

7 a) N. Arai, N. Saito, H. Nishiyama, Y. Inoue, K. Domen, K. Sato, *Chem. Lett.* **2006**, *35*, 796. b) N. Arai, N. Saito, H. Nishiyama, K. Domen, K. Sato, Y. Inoue, *Catal. Today* **2007**, in press.

8 H. Schulz, K. H. Thiemann, *Solid State Commun.* **1977**, *23*, 815.

9 a) S. Nakamura, T. Mukai, M. Senoh, *Appl. Phys. Lett.* **1994**, *64*, 1687. b) S. Nakamura, *Science* **1998**, *281*, 956.

10 a) S. S. Kocha, M. W. Peterson, D. J. Arent, J. M. Redwing, M. A. Tischler, J. A. Turner, *J. Electrochem. Soc.* **1995**, *142*, L238. b) J. D. Beach, R. T. Collins, J. A. Turner,

J. Electrochem. Soc. **2003**, *150*, A899.

11 N. H. Tran, W. J. Houschuh, R. N. Lamb, L. J. Lai, Y. W. Yang, *J. Phys. Chem. B* **2003**, *107*, 9256.

12 M. Dinescu, P. Verardi, C. Boulmer-Leborgne, C. Gerardi, L. Mirenghi, V. Sandu, *Appl. Surf. Sci.* **1998**, *127–129*, 559.

13 Y. G. Yang, H. L. Ma, C. S. Xue, X. T. Hao, H. Z. Zhuang, J. Ma, *Physica B* **2003**, *325*, 230.

14 a) G. Yu, G. Wang, H. Ishikawa, M. Umeno, T. Soga, T. Egawa, J. Watanabe, T. Jimbo, *Appl. Phys. Lett.* **1997**, *70*, 3209. b) I. K. Shmagin, J. F. Muth, J. H. Lee, R. M. Kolbas, C. M. Balkas, Z. Sitar, R. F. Davis, *Appl. Phys. Lett.* **1997**, *71*, 455.

15 Quantum efficiencies were estimated using several cutoff filters. Calculations were based on the number of incident photons in each wavelength region. Each value is plotted at the mid-point between two cutoff wavelengths, and the quantum efficiencies given in Fig. 7 represent the average with respect to those two wavelengths.

16 A. Ishikawa, T. Takata, J. N. Kondo, M. Hara, K. Domen, *J. Phys. Chem. B* **2004**, *108*, 11049.